Appendix A.27:

Avondale Park – VsVp 57187

Table 1: Site Description for Avondale Park (VsVp 57187).

Attribute	Yes/No			Description/Date	Symbol in Figure 1
	10-m Buffer	20-m Buffer	50-m Buffer		
Near a body of surface water or other free face features?	No	No	No	The center of the site is 370 m to the S from the Avon River that runs in the E-W direction. The Avon River is also 620 m to the W of the center of the site and here it runs in the S-N direction. The height of the free face is ~ 1.5 m.	NA
Lateral spreading observed during the CES?	No	No	No	No lateral spreading was observed by the mapping team.[1]	NA
Nearby buildings or structures?	No	Yes	Yes	Building coverage of the 10-m, 20-m, and 50-m buffers is 3% and 12%, respectively. The buildings are in the SW and SE quadrants of the two buffers.	White Fill + Brown Outline
Sloping land?	No	No	No	Flat land, open field + residential area	NA
Step changes in the ground surface?	No	No	No	NA	NA
Retaining walls?	No	No	No	NA	NA
Vegetation?	No	Yes	Yes	Trees and bushes cover 13% of both the 20- and 50-m buffers. They are in the SW and SE quadrants of the two buffers.	White Fill + Green Outline
Anthropogenic changes to the site between the LiDAR surveys?	Yes	Yes	Yes	Earthwork was performed in the open field between 16 Jun 2011 and Apr 2012, affecting all buffers. Building removal in the SW quadrant of the 50-m buffer occurred between Mar 2014 and Aug 2014.	Building Removal: Orange Crossline
Other important factors?	No	No	No	NA	NA

Notes: Buffer is the area within a circle of a specified radius with CPT investigations done at its center (172.690763°, -43.505496°); The Feb 2012 and Oct 2015 LiDAR surveys should not be considered in the settlement assessment due to the anthropogenic changes.

[1] Canterbury Geotechnical Database. (2012). "Observed Ground Crack Locations", Map Layer CGD0400 - 23 July 2012, retrieved July 09, 2018 from https://canterburygeotechnicaldatabase.projectorbit.com/

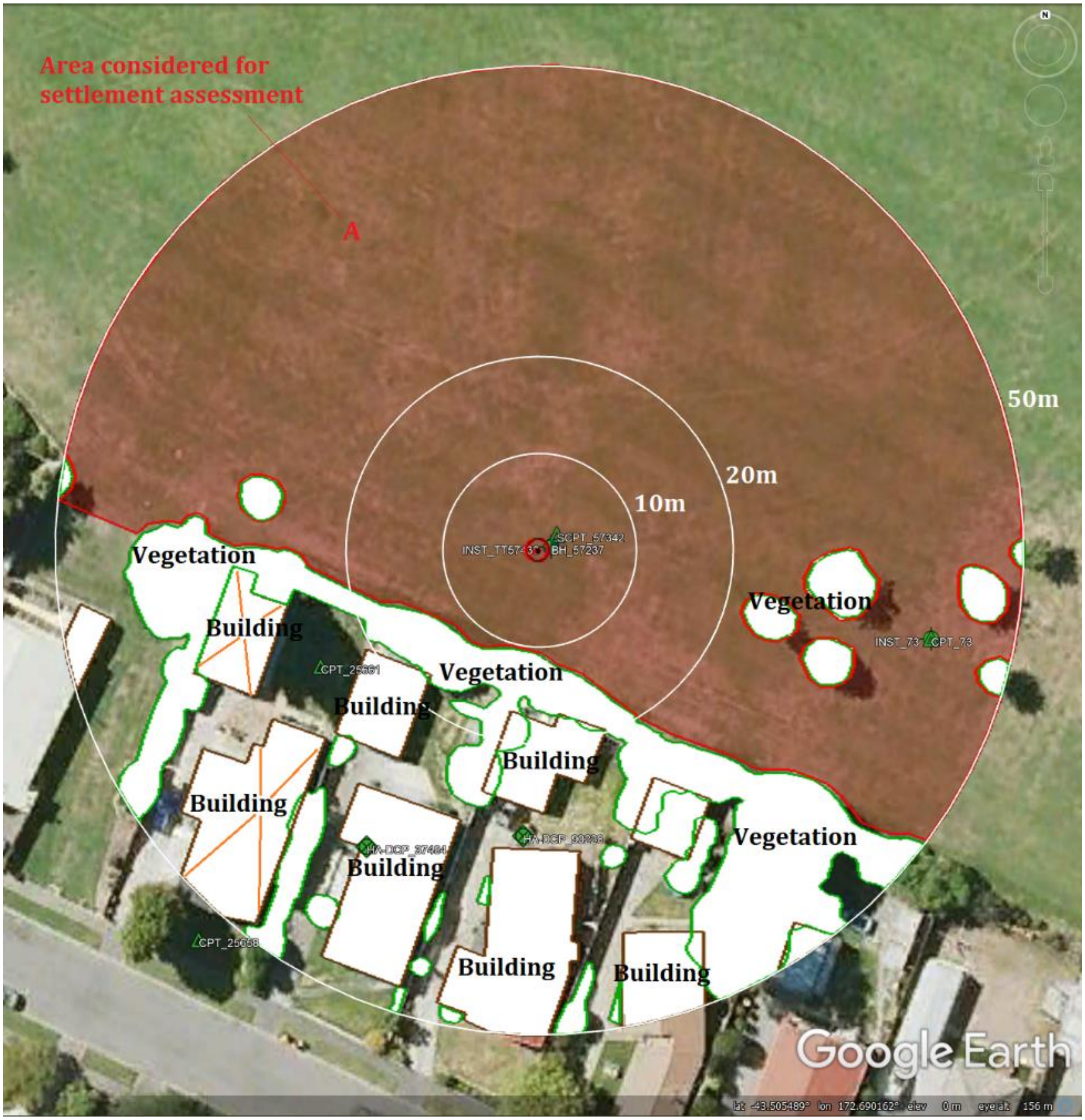

Figure 1: Site plan with areas where ejecta-induced settlement is considered.

Note 1: Patch A (outlined in red) in the free field was selected for settlement assessment as an area free of vegetation and structures. Other important factors considered in its selection were its proximity a CPT, a property subjected to addition and/or demolition of a structure, front yard/backyard alterations (e.g., ploughing, rubble, scrap), and aerial distribution of sediment ejecta. The LiDAR-based settlement analyses were not performed for any earthquake event due to the evident absence of ejecta from the site for the Sep-10 EQ, LiDAR flight errors, overestimation by liquefaction triggering procedures, and anthropogenic changes.

Table 2: LiDAR flight error adjustments, global adjustments for the difference between average LiDAR point elevations and benchmark survey elevations, and vertical tectonic movement adjustments.

	Adjustments (mm)		
Earthquake Event(s)	LiDAR Flight Error	Global Offset[2]	Tectonic Vertical Movement
Sep-10	-100	-3	0
Feb-11	+100	16	-40
Jun-11	0	38	-48
Dec-11	0	-65	0
CES	0	-14	-88
Any LiDAR survey affected by ejecta?			No

Note: The negative sign indicates the subtraction from the ground surface subsidence, while the positive sign indicates the addition to the ground surface subsidence.

Table 3a: LiDAR Measurement Error for Patch A.

Surveys	Buffer	Area Averaged Difference Indicating Repeat Measurement Error (mm)	$\sigma^{*}_{\text{individual LiDAR points}}$ (mm)	%Reduction in σ due to Area Averaging of LiDAR Points
Post Feb 2011: Mar 2011 and May 2011	10-m	ND	59	[ND,ND]
	20-m	ND		
	50-m	ND		
Post Dec 2011: Feb 2012 and Oct 2015	10-m	ND	70	[ND,ND]
	20-m	ND		
	50-m	ND		

*Standard deviation; ND = Not determined.

[2] Russell, J., & van Ballegooy, S. (2015). *Canterbury Earthquake Sequence: Increased liquefaction vulnerability assessment methodology*. New Zealand: Tonkin & Taylor Ltd.

Table 4: Ground surface subsidence adjustments due to LiDAR measurement error for Patch A (10-m buffer).

Earthquake Event(s)	$\sigma_{pre\text{-}EQ\ LiDAR\ survey}$ (mm)	$\sigma_{post\text{-}EQ\ LiDAR\ survey}$ (mm)	σ_{total} (mm)	Area Average Adjusted σ (mm) **
Sep-10	158	56	134	ND
Feb-11	56	59	59	ND
Jun-11	59	61	62	ND
Dec-11	61	70	87	ND
CES	158	70	124	ND

**Based on the highest %Reduction in Table 3a.

Table 5: Raw liquefaction-related ground surface subsidence using original LiDAR points for Patch A.

	Average Ground Surface Subsidence (mm)		
Earthquake Event(s)	10-m Buffer	20-m Buffer	50-m Buffer
Sep-10	ND	ND	ND
Feb-11	ND	ND	ND
Jun-11	ND	ND	ND
Dec-11	ND	ND	ND
CES	ND	ND	ND

ND = Not determined.

Table 6: Corrected liquefaction-related ground surface subsidence using original LiDAR points for Patch A with the calculated adjustments in Table 2.

	Average Calculated Ground Surface Subsidence (mm)		
Earthquake Event(s)	10-m Buffer	20-m Buffer	50-m Buffer
Sep-10	ND	ND	ND
Feb-11	ND	ND	ND
Jun-11	ND	ND	ND
Dec-11	ND	ND	ND
CES	ND	ND	ND

Notes: Plus/minus values are same as those in Table 4a, but rounded to the nearest 25; Positive overall values indicate ground surface subsidence, while negative overall values indicate ground surface uplift; ND = Not determined.

Table 7: Corrected liquefaction-related ground surface subsidence for Patch A using LiDAR DEMs.

	Estimated Ground Surface Subsidence (mm)								
	10-m Buffer			20-m Buffer			50-m Buffer		
Earthquake Event(s)	16th %ile	50th %ile	84th %ile	16th %ile	50th %ile	84th %ile	16th %ile	50th %ile	84th %ile
Sep-10	<50	<50	50	<50	<50	50	<50	<50	50
Feb-11	200	250	250	200	250	250	150	250	350
Jun-11	<50	50	50	<50	50	50	<50	50	50
Dec-11	ND	ND	ND	ND	ND	ND	ND	ND	ND
CES	ND	ND	ND	ND	ND	ND	ND	ND	ND

Notes: These percentiles are not the exact statistical measures; they indicate the spatial variability of ground surface subsidence; ND = Not determined due to the anthropogenic changes following the Jun-11 earthquake.

Table 8a: Ejecta-Induced settlement for the top 20 m of the soil profile for Patch A (10-m buffer) for the 50th %ile PGA, P_L=50%, and C_{FC}=0.13 using BI-2014, ZRB-2002, and I_C cutoff of 2.6.

Earthquake Event(s)	M_W	PGA (g)	Depth to Groundwater (m)	S_T (mm)	S_{V1D} (mm)	$S_{E,L}$ (mm)
Sep-10	7.1	0.18	1.5	ND	41±20	ND
Feb-11	6.2	0.37	1.5	ND	154±50	ND
Jun-11	6.2	0.25	0.5	ND	124±25	ND
Dec-11	6.1	0.30	1.5	ND	122±50	ND

Notes: S_T = Total settlement (Table 6); S_{V1D} = Average vertical settlement due to volumetric compression using Boulanger and Idriss (2014) (BI-2014), Zhang et al. (2002) (ZRB-2002) procedures and de Greef and Lengkeek (2018) thin-layer correction; $S_{E,L}$ = Ejecta-induced settlement as the difference between the LiDAR-based S_T and S_{V1D}; ND = Not determined.

Table 8b: Ejecta-Induced settlement for the top 20 m of the soil profile for Patch A (20-m buffer) for the 50th %ile PGA, P_L=50%, and C_{FC}=0.13 using BI-2014, ZRB-2002, and I_C cutoff of 2.6.

Earthquake Event(s)	M_W	PGA (g)	Depth to Groundwater (m)	S_T (mm)	S_{V1D} (mm)	$S_{E,L}$ (mm)
Sep-10	7.1	0.18	1.5	ND	61±20	ND
Feb-11	6.2	0.37	1.5	ND	168±50	ND
Jun-11	6.2	0.25	0.5	ND	144±25	ND
Dec-11	6.1	0.30	1.5	ND	138±50	ND

Notes: S_T = Total settlement (Table 6); S_{V1D} = Average vertical settlement due to volumetric compression using Boulanger and Idriss (2014) (BI-2014), Zhang et al. (2002) (ZRB-2002) procedures and de Greef and Lengkeek (2018) thin-layer correction; $S_{E,L}$ = Ejecta-induced settlement as the difference between the LiDAR-based S_T and S_{V1D}; ND = Not determined.

Table 8c: Ejecta-Induced settlement for the top 20 m of the soil profile for Patch A (50-m buffer) for the 50th %ile PGA, P_L=50%, and C_{FC}=0.13 using BI-2014, ZRB-2002, and I_C cutoff of 2.6.

Earthquake Event(s)	M_W	PGA (g)	Depth to Groundwater (m)	S_T (mm)	S_{V1D} (mm)	$S_{E,L}$ (mm)
Sep-10	7.1	0.18	1.5	ND	60±20	ND
Feb-11	6.2	0.37	1.5	ND	170±50	ND
Jun-11	6.2	0.25	0.5	ND	145±25	ND
Dec-11	6.1	0.30	1.5	ND	140±50	ND

Notes: S_T = Total settlement (Table 6); S_{V1D} = Average vertical settlement due to volumetric compression using Boulanger and Idriss (2014) (BI-2014), Zhang et al. (2002) (ZRB-2002) procedures and de Greef and Lengkeek (2018) thin-layer correction; $S_{E,L}$ = Ejecta-induced settlement as the difference between the LiDAR-based S_T and S_{V1D}; ND = Not determined.

Note 2: The uncertainty for volumetric settlement was derived based on the sensitivity of volumetric settlement to PGA, C_{FC}, and P_L for each earthquake event for VsVp 57203 *Shirley Intermediate School* and CC LIQ 1 – CPT 5586 – *Vivian St* sites. Taking the 50th percentile as the baseline case, the minimum and maximum values corresponding to the difference between the 25th percentile and the 50th percentile and the 75th percentile and the 50th percentile were determined. The arithmetic mean of the range of the minimum and maximum difference was evaluated for each patch at the two sites. The maximum arithmetic mean for each earthquake event was rounded to the nearest five and used as the uncertainty value. Accordingly, the 1-D volumetric settlement uncertainties of ±20, ±50, ±25, and ±50 mm for the Sep-10, Feb-11, Jun-11, and Dec-11 earthquake events, respectively, were used for all sites in this study.

Table 9a: Coverage area and height of ejecta estimates for Patch A (10-m buffer) using photographs.

EQ Event	$H_{E,thick1}$ (mm)	$A_{E,thick1}$ (m^2)	$H_{E,thick2}$ (mm)	$A_{E,thick2}$ (m^2)	$H_{E,thin1}$ (mm)	$A_{E,thin1}$ (m^2)	$H_{E,thin2}$ (mm)	$A_{E,thin2}$ (m^2)	A_T (m^2)
Sep-10	0	0	0	0	0	0	0	0	314
Feb-11	0	0	0	0	20-40	118	10-20	24.6	314
Jun-11	0	0	0	0	60-100	25.1	10-20	1.1	314
Dec-11	0	0	0	0	0	0	3-6	17.1	161*

Notes: $A_{E,thick/thin}$ = Coverage area of thick/thin ejecta layers; $H_{E,thick/thin}$ = Lower-upper estimate of height of thick/thin ejecta layers; A_T= Total assessment area of a buffer being considered; * indicates reduction in A_T due to the presence of construction equipment.

Table 9b: Coverage area and height of ejecta estimates for Patch A (20-m buffer) using photographs.

EQ Event	$H_{E,thick1}$/ $H_{E,cone}$ (mm)	$A_{E,thick1}$/ $A_{E,cone}$ (m^2)	$H_{E,thick2}$ (mm)	$A_{E,thick2}$ (m^2)	$H_{E,thin1}$ (mm)	$A_{E,thin1}$ (m^2)	$H_{E,thin2}$ (mm)	$A_{E,thin2}$ (m^2)	A_T (m^2)
Sep-10	0	0	0	0	0	0	0	0	1035
Feb-11	80-160	43.7	40-80	41.8	20-40	264	10-20	175	1035
Jun-11	0	0	0	0	60-100	46.9	10-20	1.1	1026*
Dec-11	200-300	7.4	70-140	0.4	40-60	8.5	10-20 3-6	1.0 30.8	733*

Notes: $A_{E,thick/thin}$ = Coverage area of thick/thin ejecta layers; $H_{E,\ thick/thin}$ = Lower-upper estimate of height of thick/thin ejecta layers; $A_{E,cone}$ = Coverage area of conically shaped ejecta for the Dec-11 EQ; $H_{E,cone}$ = Lower-upper estimate height of conically shaped ejecta for the Dec-11 EQ; $A_{E,cone}$ = Coverage area of conically shaped ejecta for the Dec-11 EQ; $H_{E,cone}$ = Lower-upper estimate height of conically shaped ejecta for the Dec-11 EQ; A_T= Total assessment area of a buffer being considered; * indicates reduction in A_T due to the presence of ejecta piles from the Feb-11 EQ (for the Jun-11 EQ) and the construction equipment (for the Dec-11 EQ).

Table 9c: Coverage area and height of ejecta estimates for Patch A (50-m buffer) using photographs.

EQ Event	$H_{E,thick1}$/ $H_{E,cone}$ (mm)	$A_{E,thick1}$ / $A_{E,cone}$ (m^2)	$H_{E,thick2}$ (mm)	$A_{E,thick2}$ (m^2)	$H_{E,thin1}$ (mm)	$A_{E,thin1}$ (m^2)	$H_{E,thin2}$ (mm)	$A_{E,thin2}$ (m^2)	A_T (m^2)
Sep-10	0	0	0	0	0	0	0	0	4905
Feb-11	80-160	510	40-80	249	20-40	488	10-20	700	4905
Jun-11	0	0	0	0	60-100	468	10-20	17.0	4822*
Dec-11	200-300	7.4	70-140	169	40-60	169	10-20 3-6	110 45.7	4572*

Notes: $A_{E,thick/thin}$ = Coverage area of thick/thin ejecta layers; $H_{E,\ thick/thin}$ = Lower-upper estimate of height of thick/thin ejecta layers; A_T= Total assessment area of a buffer being considered; $A_{E,cone}$ = Coverage area of conically shaped ejecta for the Dec-11 EQ; $H_{E,cone}$ = Lower-upper estimate height of conically shaped ejecta for the Dec-11 EQ; * indicates reduction in A_T due to the presence of ejecta piles from the Feb-11 EQ (for the Jun-11 EQ) and the construction equipment (for the Dec-11 EQ).

Note 3: The values in Table 9 correspond to the coverage area of ejecta outlined in aerial photographs (Figures 36-38) and the lower and upper estimates of ejecta height based on geometrical approximations, ground photographs (Figure 39), and EQC LDAT property inspection reports. The ejecta-induced settlement using photographs and engineering judgment, $S_{E,P}$, is estimated as

$$S_{E,P} = \frac{\sum_{i=1}^{a} A_{E,thick,i} * H_{E,thick,i} + \sum_{j=1}^{b} A_{E,thin,j} * H_{E,thin,j} + \frac{1}{3}\sum_{m=1}^{e} A_{E,cone,m} * H_{E,cone,m}}{A_T}$$

$$= \frac{\sum_{i=1}^{a} V_{E,thick,i} + \sum_{j=1}^{b} V_{E,thin,j} + \sum_{m=1}^{e} V_{E,cone,m}}{A_T}$$

where

- $A_{E,thick,i}$ and $H_{E,thick,i}$ are the area and the height of a thick ejecta layer, respectively;
- $A_{E,thin,j}$ and $H_{E,thin,j}$ are the area and the height of a thin ejecta layer, respectively;

- $A_{E,cone,m}$ and $H_{E,cone,m}$ are the aerea and the height of a conically shaped ejecta, respectively;
- A_T is the total assessment area for a buffer being considered (Figure 1).

Table 10: Ejecta-induced settlement estimates for Patch A based on photographs.

Earthquake Event	Patch A (10-m buffer)		Patch A (20-m buffer)		Patch A (50-m buffer)	
	$S_{E,P,lower}$ (mm)	$S_{E,P,upper}$ (mm)	$S_{E,P,lower}$ (mm)	$S_{E,P,upper}$ (mm)	$S_{E,P,lower}$ (mm)	$S_{E,P,upper}$ (mm)
Sep-10	0	0	0	0	0	0
Feb-11	8	17	12	24	14	28
Jun-11	5	8	3	5	6	10
Dec-11	≈0	1	1	2	4	8

Note: $S_{E,P,lower}$ and $S_{E,P,upper}$ correspond to lower and upper estimates of $S_{E,P}$, respectively.

Table 11: Best final estimates of ejecta-induced settlement for Patch A.

EQ Event	Patch A (10-m buffer)			Patch A (20-m buffer)			Patch A (50-m buffer)		
	$S_{E,L}$ (mm)	$S_{E,P}$ (mm)	$S_{E,final}$ (mm)	$S_{E,L}$ (mm)	$S_{E,P}$ (mm)	$S_{E,final}$ (mm)	$S_{E,L}$ (mm)	$S_{E,P}$ (mm)	$S_{E,final}$ (mm)
Sep-10	ND	0	0	ND	0	0	ND	0	0
Feb-11	ND	13±4	15±5	ND	18±6	20±5	ND	21±7	20±10
Jun-11	ND	6.5±1.5	5±5	ND	4±1	5±5	ND	8±2	10±5
Dec-11	ND	0.5±0.5	<5	ND	1.5±0.5	<5	ND	6±2	5±5

Notes: $S_{E,L}$ = Ejecta-induced settlement based on LiDAR data reported in Table 8; $S_{E,P}$ = Median ejecta-induced settlement for the range of values reported in Table 10; $S_{E,final}$ = Best final estimate of ejecta-induced settlement rounded to the nearest 5; Final plus/minus values are also rounded to the nearest 5; ND = Not determined.

Note 4:

- $S_{E,final}$ is based solely on $S_{E,P}$ for all EQ events.
- The Avondale Park site is in the apparent zone of higher ground surface subsidence for the Sep-10 EQ and the apparent zone of lower ground surface subsidence for the Feb-11 EQ (the underestimate of the ground surface elevation by the Sep 2010 LiDAR survey). The site is in the zone of accurate LPI prediction of liquefaction severity for the Sep-10 and slight LPI overprediction of liquefaction severity for the Feb-11 EQ (Maurer et al. 2014[3]). The LDAT property inspection reports are available for nearby properties; however, no measurements of the ejecta height were taken during the inspection. A ground photograph that shows remnants of ejecta at a nearby property is available.

<u>**Summary 1**</u>**:**

The best estimate of the ejecta-induced free-field ground settlement at the Avondale Park site for the SEP 2010, FEB 2011, JUN 2011, and DEC 2011 earthquake is 0 mm, 20±10 mm, 10±5 mm, and 5±5 mm, respectively.

[3] Maurer, B. W., Green, R. A., Cubrinovski, M., & Bradley, B. A. (2014). Evaluation of the Liquefaction Potential Index for Assessing Liquefaction Hazard in Christchurch, New Zealand. *Journal of Geotechnical and Geoenvironmental Engineering*, 140(7), 04014032-1-11. doi:10.1061/(asce)gt.1943-5606.0001117

Figure 2: Location of the site.

Figure 3: Position of the site relative to nearby free-face features.

Figure 4: Position of the site relative to nearby buildings and vegetation.

Figure 5: Street view of the flat land.

Figure 6: Satellite image of the site taken in Dec 2004.

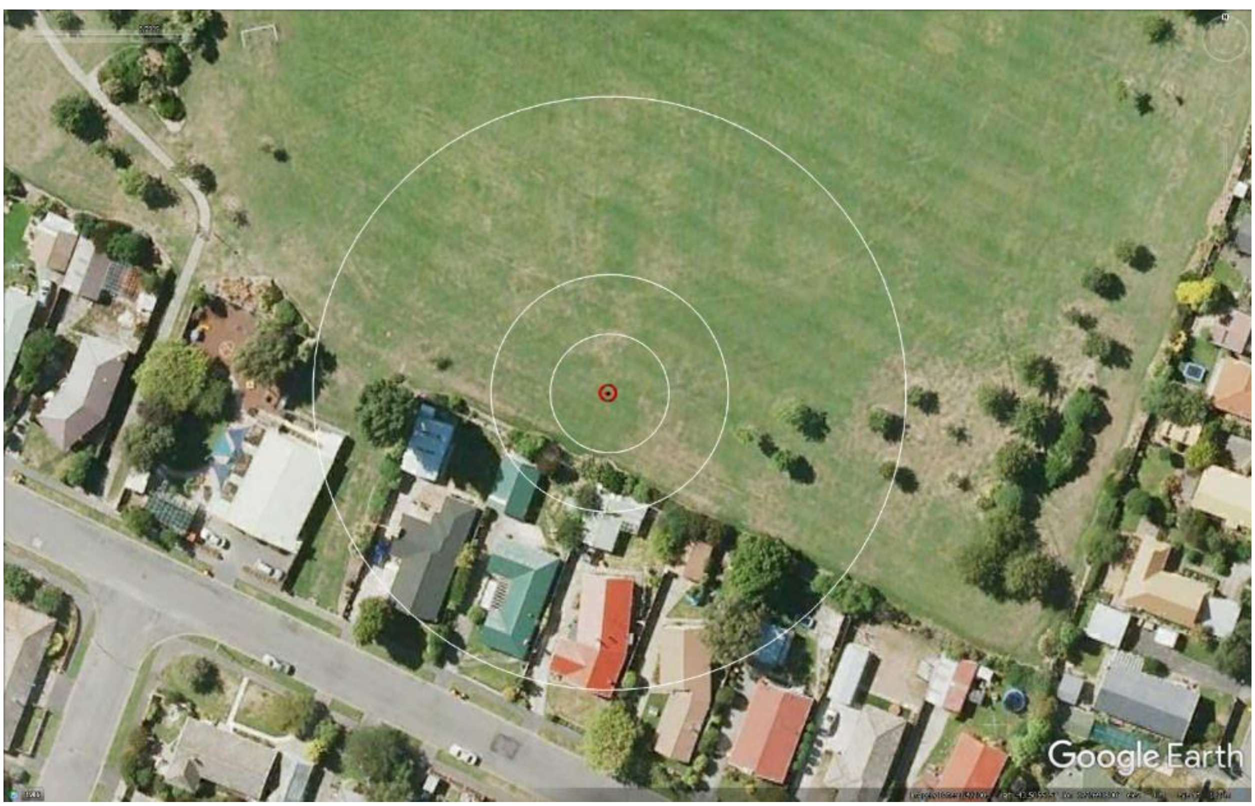

Figure 7: Satellite image of the site taken in Mar 2009.

Figure 8: Satellite image of the site taken on Sep 3, 2010.

Figure 9: Satellite image of the site taken on Sep 5, 2010.

Figure 10: Satellite image of the site taken on Feb 7, 2011.

Figure 11: Satellite image of the site taken on Feb 23, 2011.

Figure 12: Satellite image of the site taken on Feb 26, 2011.

Figure 13: Satellite image of the site taken on Mar 8, 2011.

Figure 14: Satellite image of the site taken in Apr 2012.

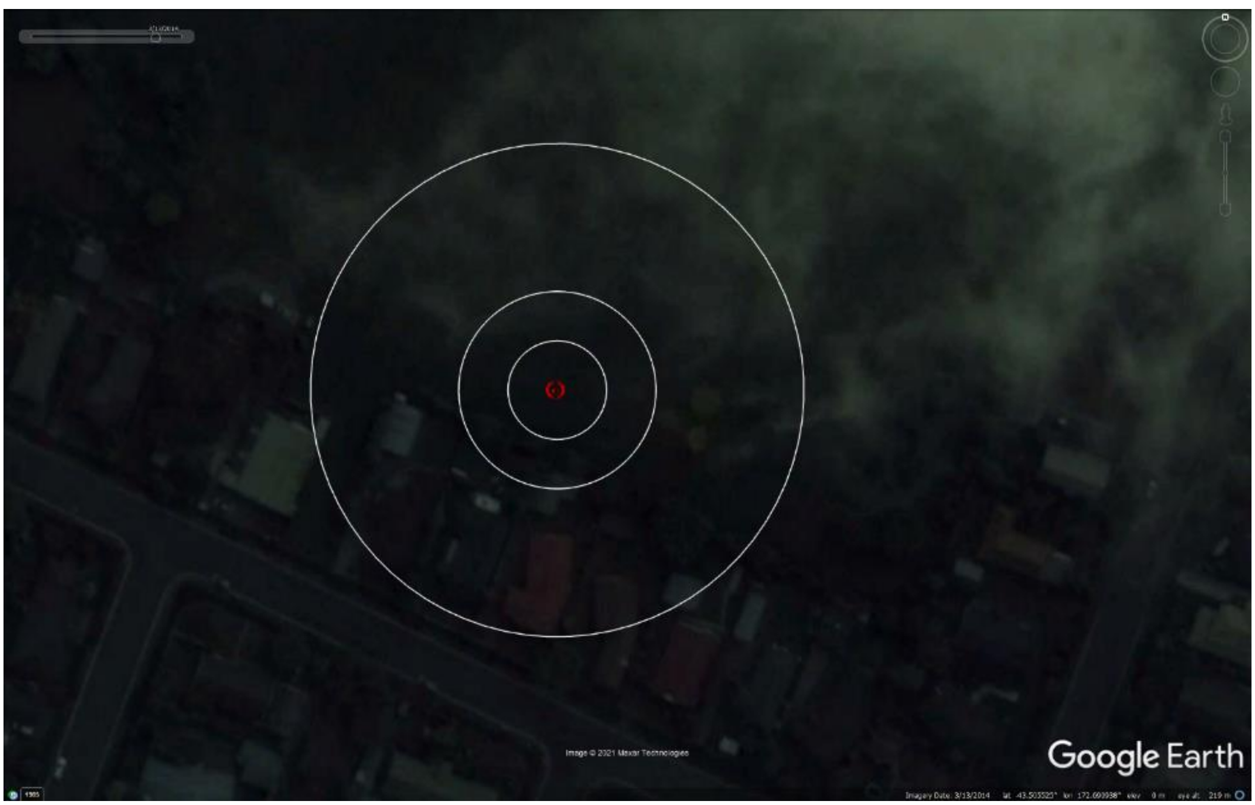

Figure 15: Satellite image of the site taken in Mar 2014.

Figure 16: Satellite image of the site taken in Aug 2014.

Figure 17: Satellite image of the site taken in Nov 2015.

Figure 18: Aerial photograph of the site taken on Sep 4, 2010.

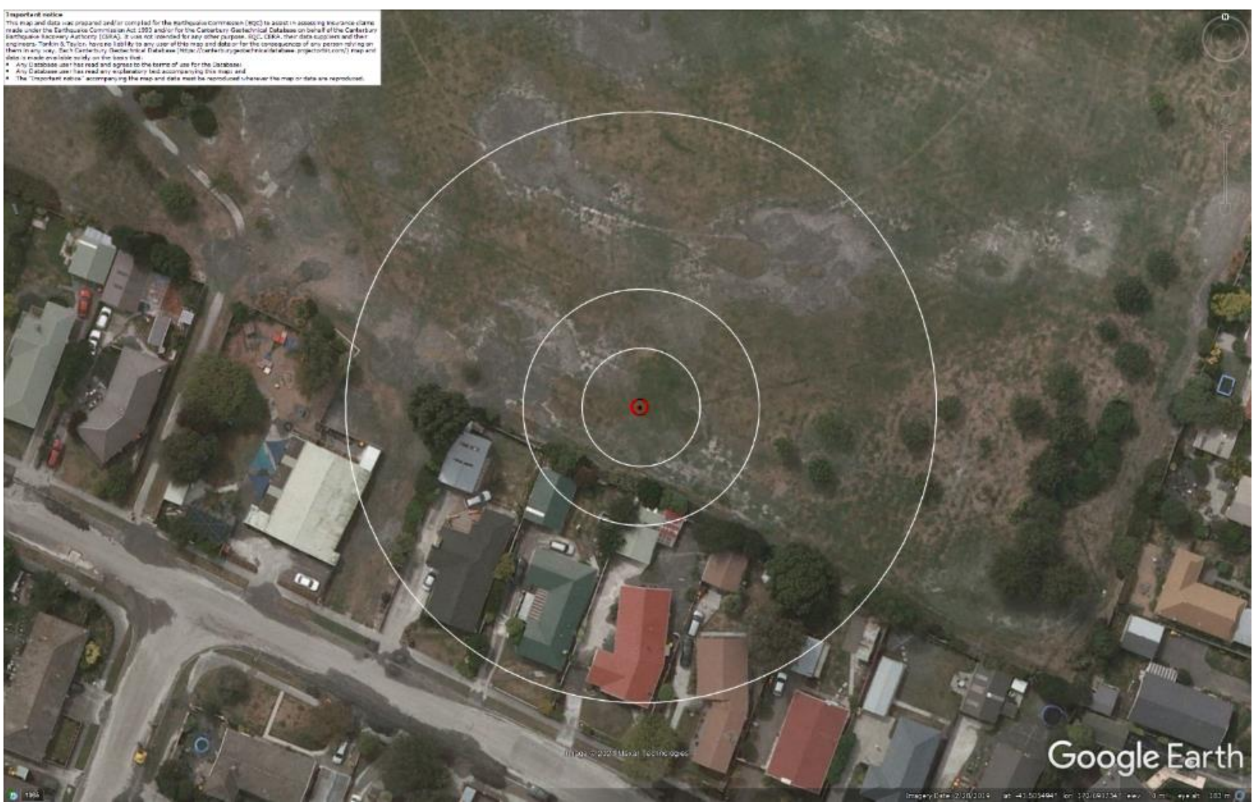

Figure 19: Aerial photograph of the site taken on Feb 24, 2011.

Figure 20: Aerial photograph of the site taken on June 14-15, 2011.

Figure 21: Aerial photograph of the site taken on June 16, 2011.

Figure 22: Aerial photograph of the site taken on Dec 24, 2011.

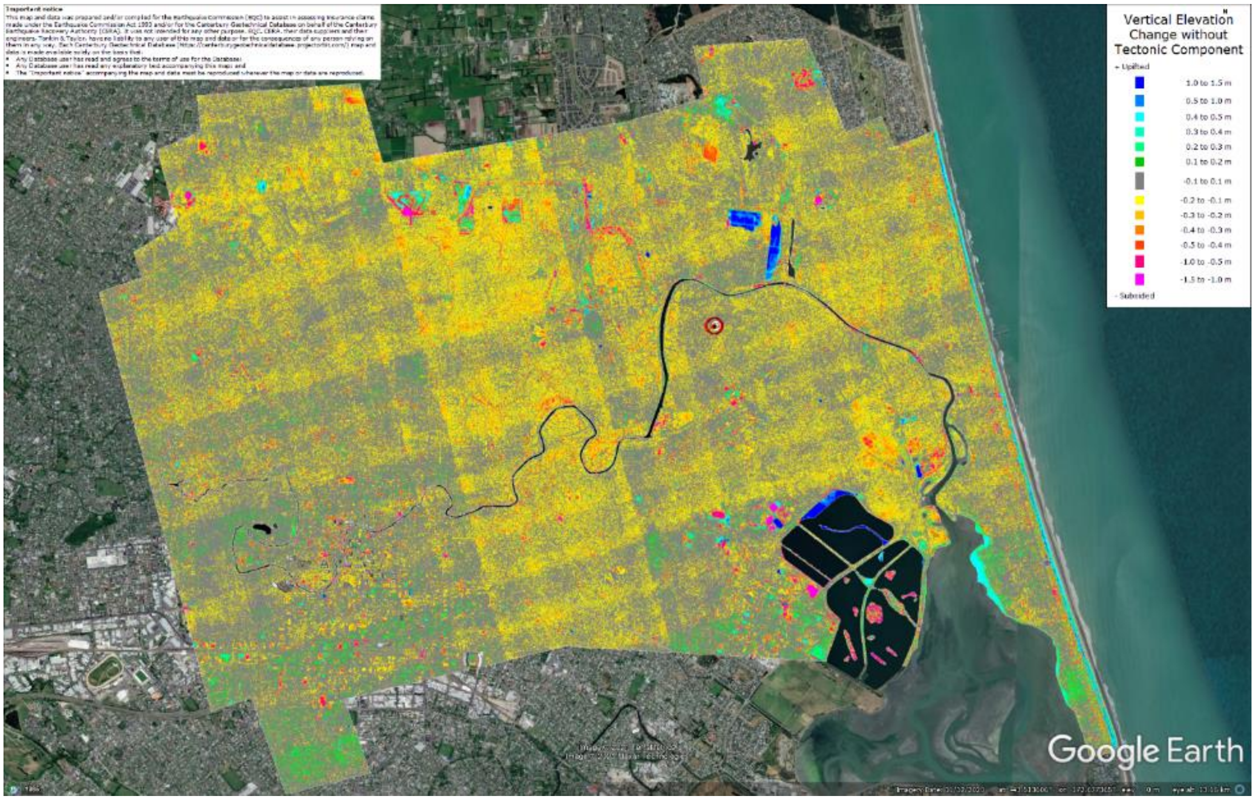

Figure 23: Vertical Ground Movements (Surface – Tectonic) for Sep 2010 Earthquake – the site is in the apparent zone of overestimated ground surface subsidence (i.e., flight error band for Sep 2010).

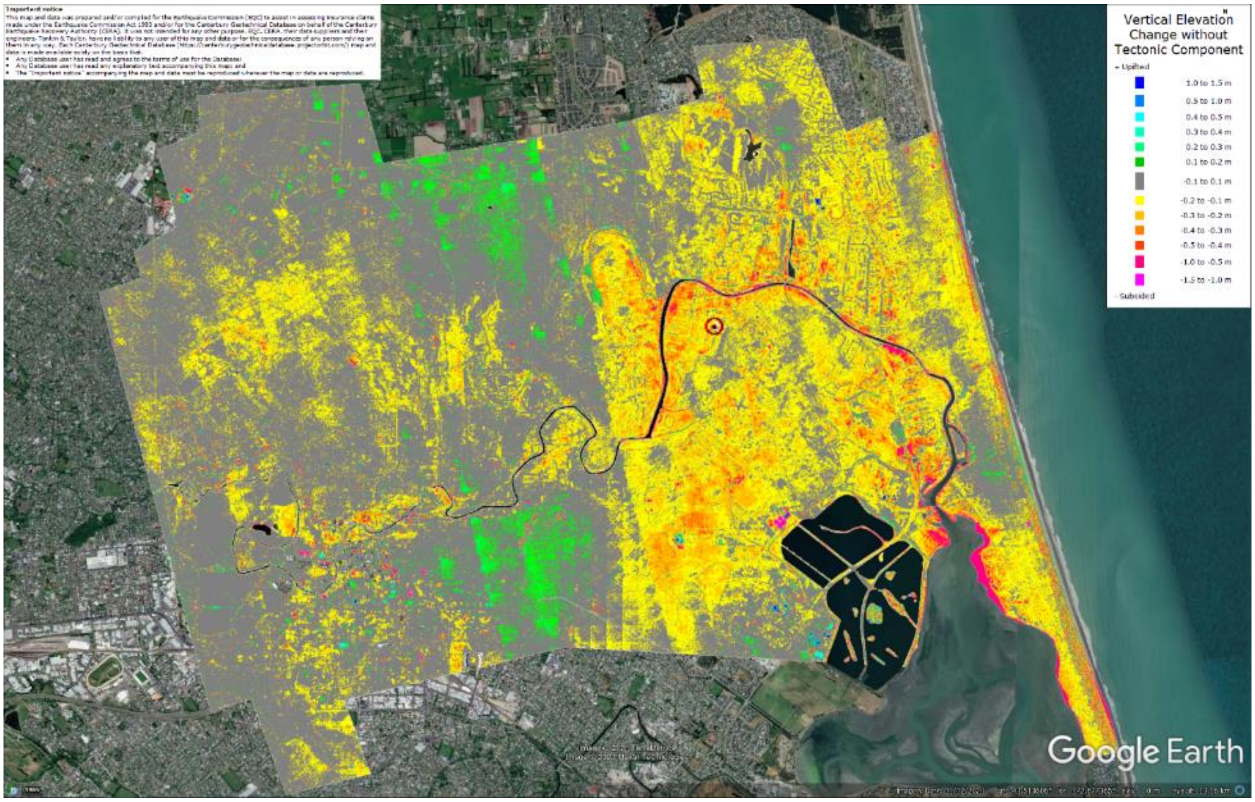

Figure 24: Vertical Ground Movements (Surface – Tectonic) for Feb 2011 Earthquake – the site is in the apparent zone of underestimated ground surface subsidence (i.e., flight error band for Sep 2010).

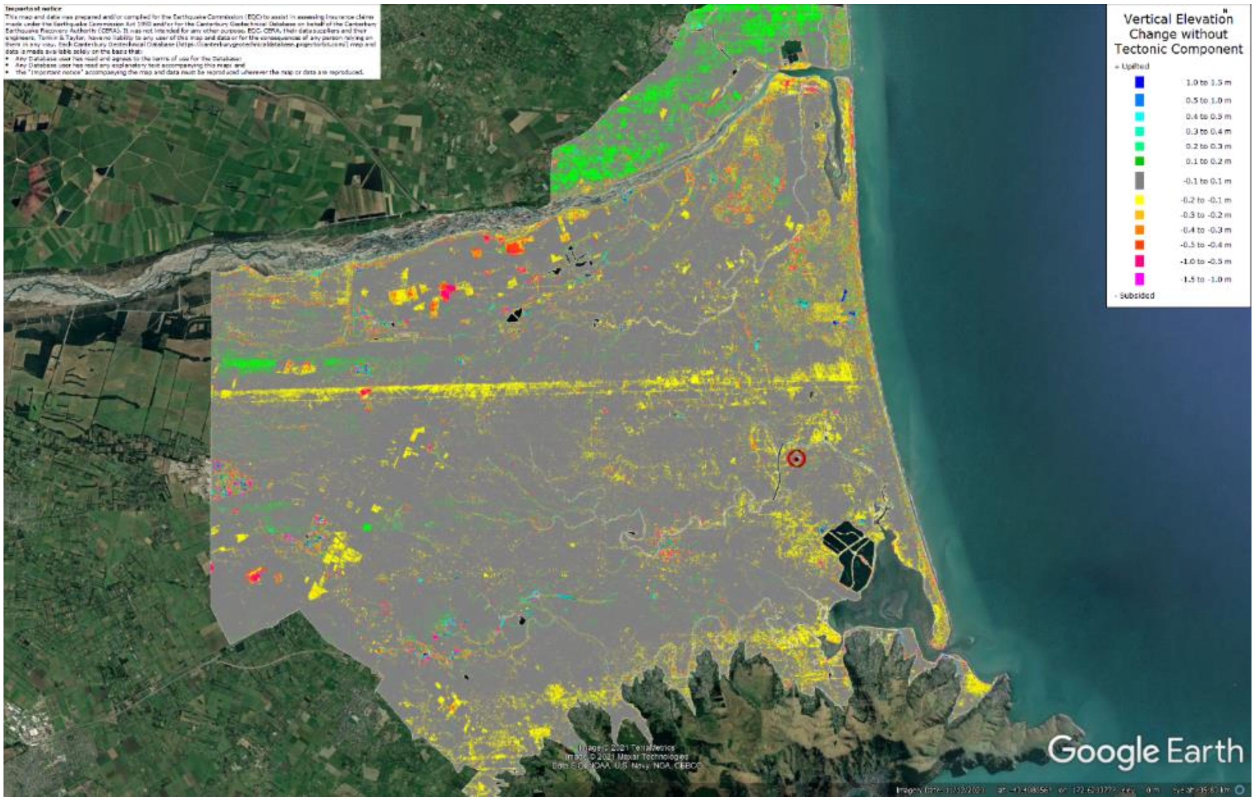

Figure 25: Vertical Ground Movements (Surface – Tectonic) for June 2011 Earthquake – the site is not in the apparent zone of overestimated or underestimated ground surface subsidence.

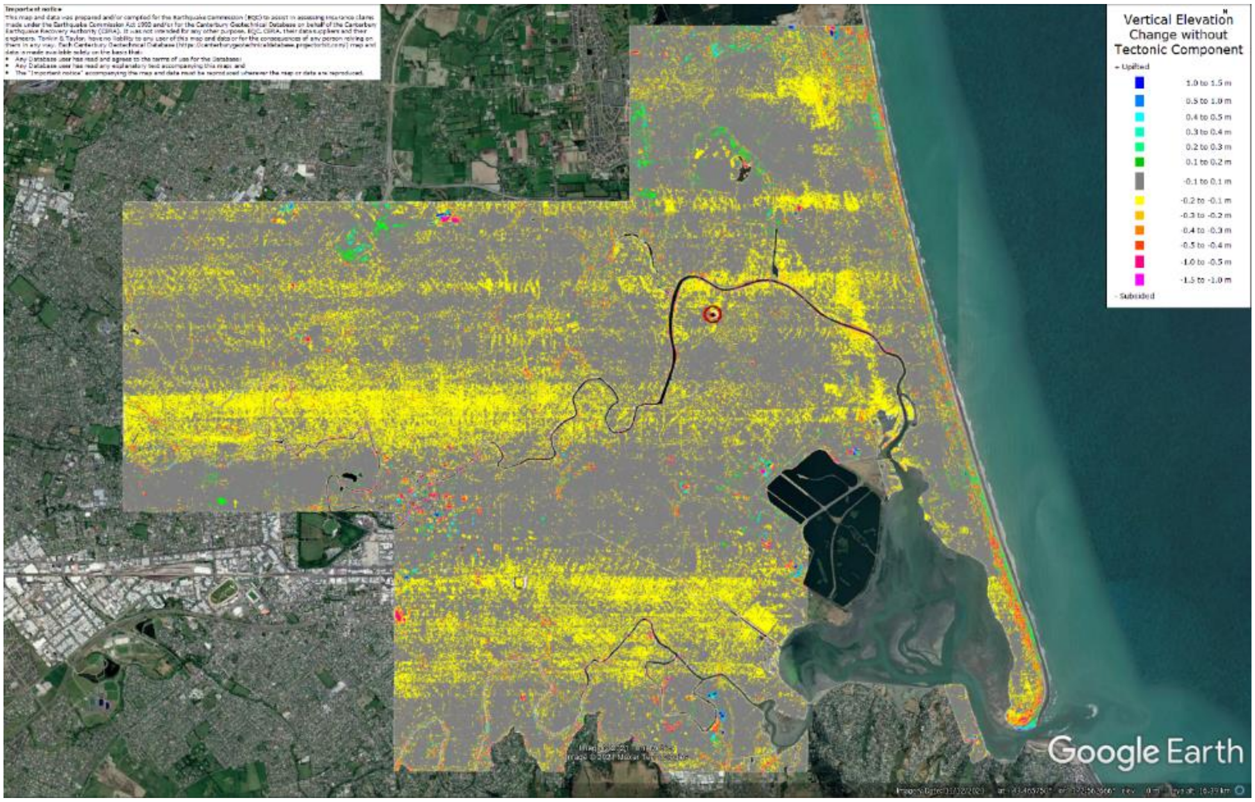

Figure 26: Vertical Ground Movements (Surface – Tectonic) for Dec 2011 Earthquake – the site is not in the apparent zone of overestimated or underestimated ground surface subsidence.

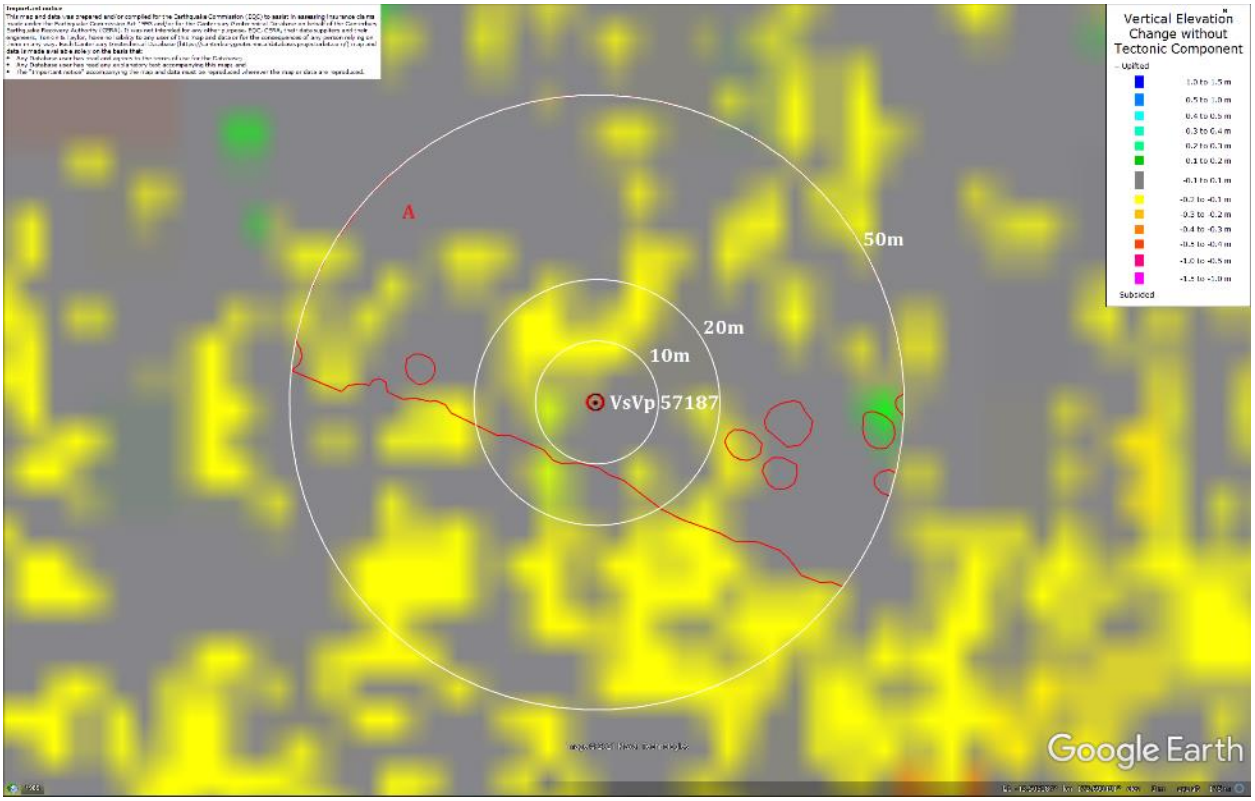

Figure 27: Ground surface subsidence without tectonic component for Sep 2010 Earthquake according to the LiDAR DEM.

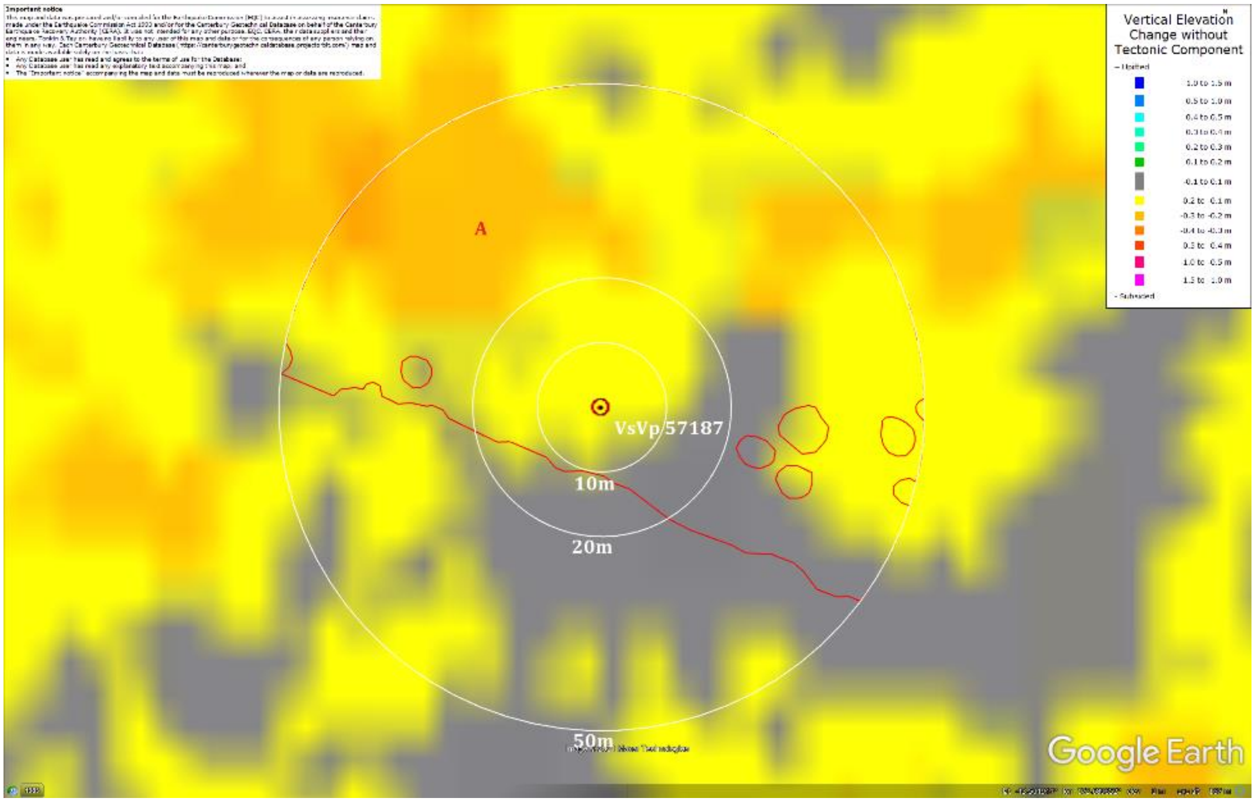

Figure 28: Ground surface subsidence without tectonic component for Feb 2011 Earthquake according to the LiDAR DEM.

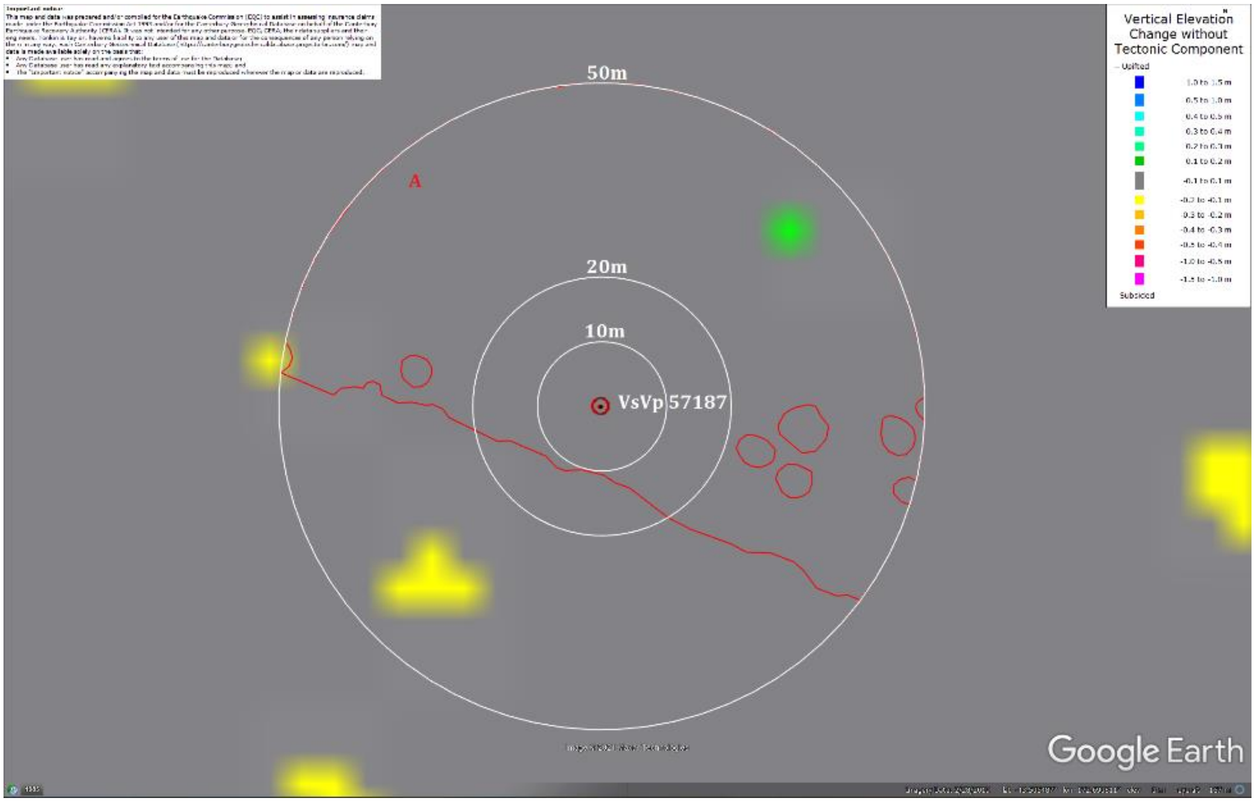

Figure 29: Ground surface subsidence without tectonic component for June 2011 Earthquake according to the LiDAR DEM.

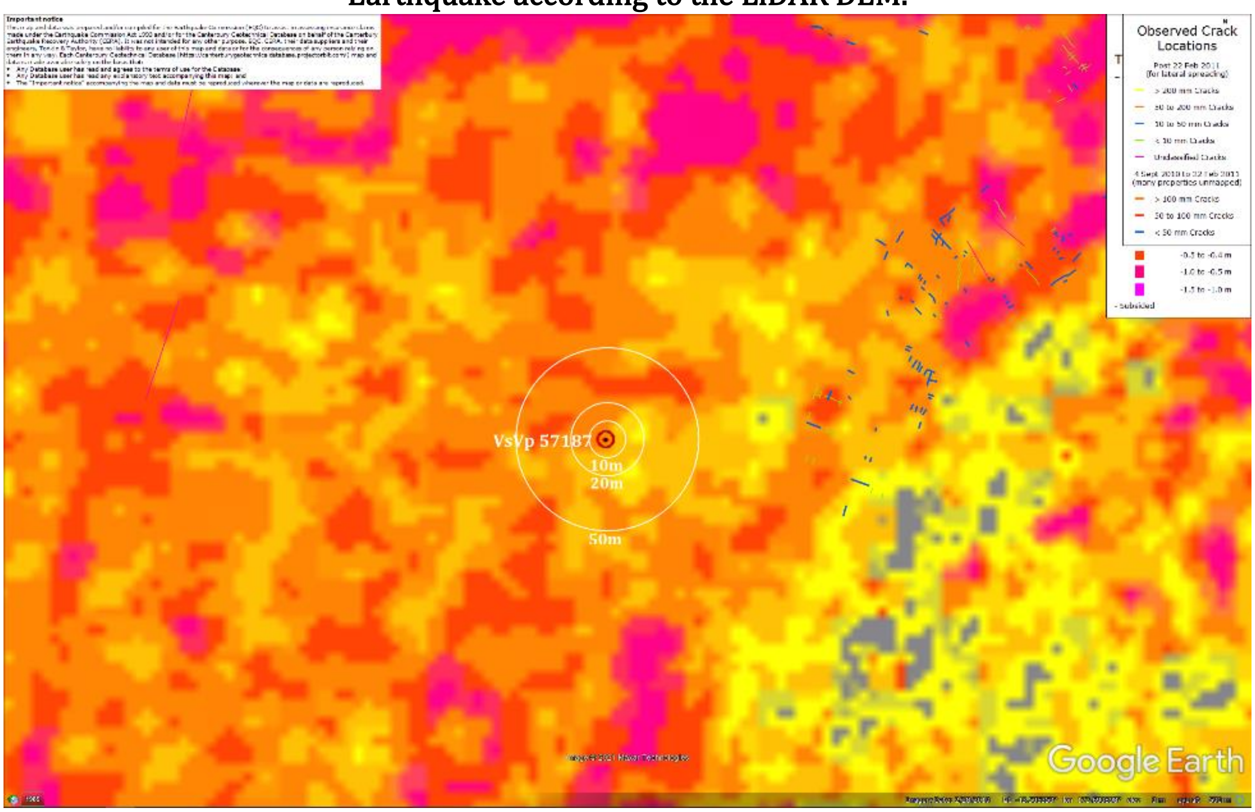

Figure 30: No lateral spreading for Canterbury Earthquake Sequence.

Figure 31: Vertical tectonic movements for Sep 2010 Earthquake.

Figure 32: Vertical tectonic movements for Feb 2011 Earthquake.

Figure 33: Vertical tectonic movements for June 2011 Earthquake.

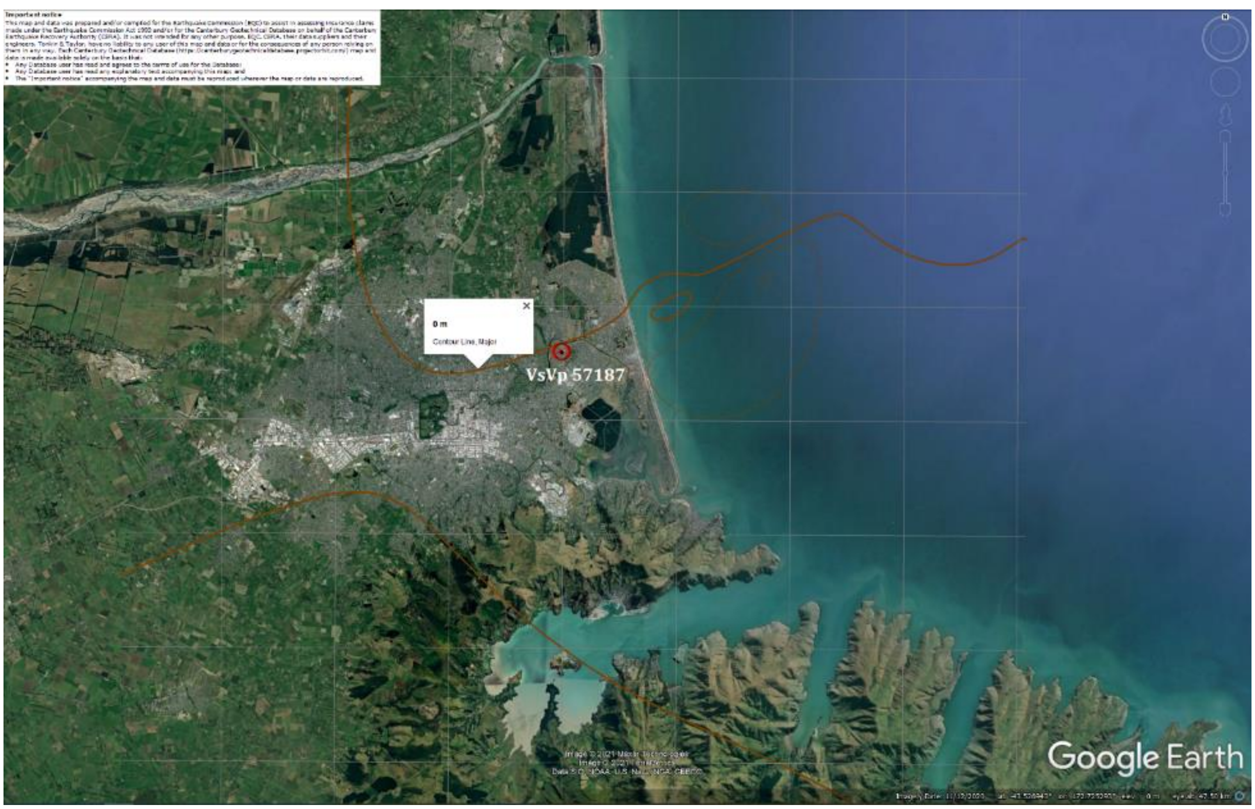

Figure 34: Vertical tectonic movements for Dec 2011 Earthquake.

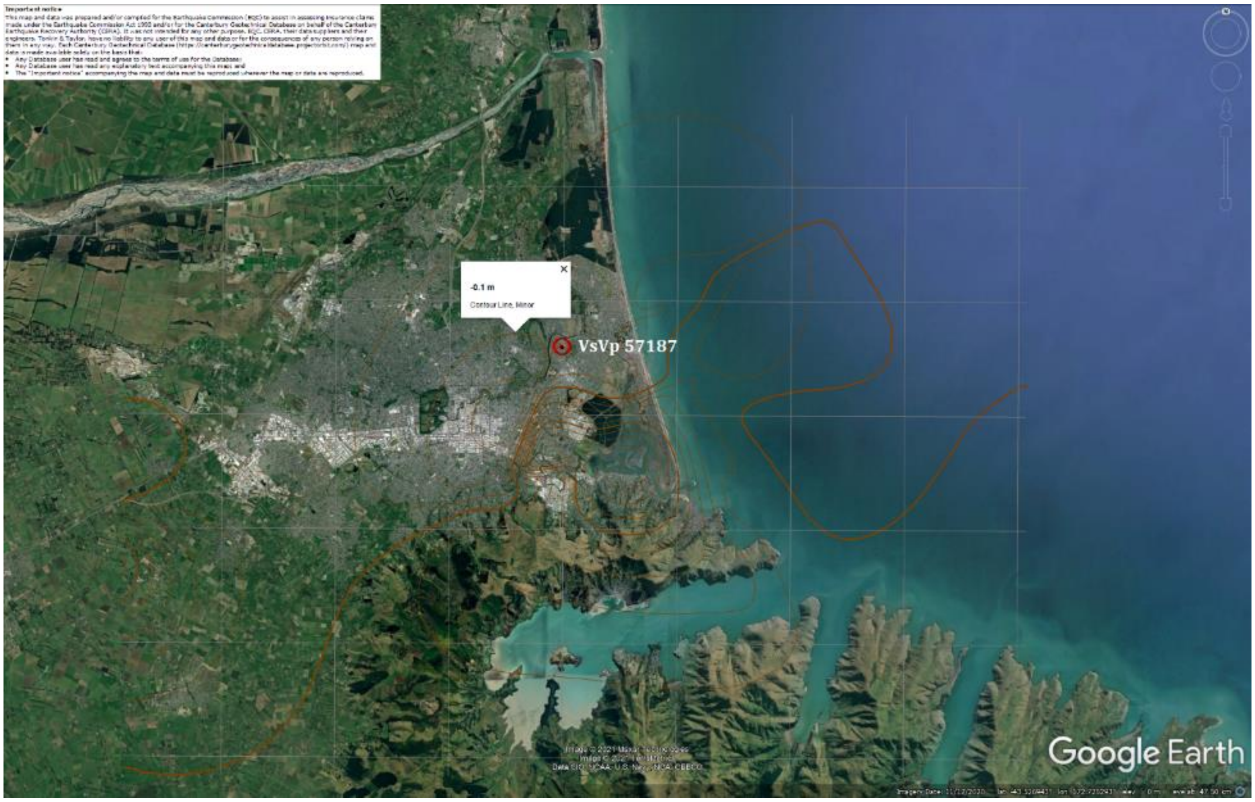

Figure 35: Vertical tectonic movements for Canterbury Earthquake Sequence.

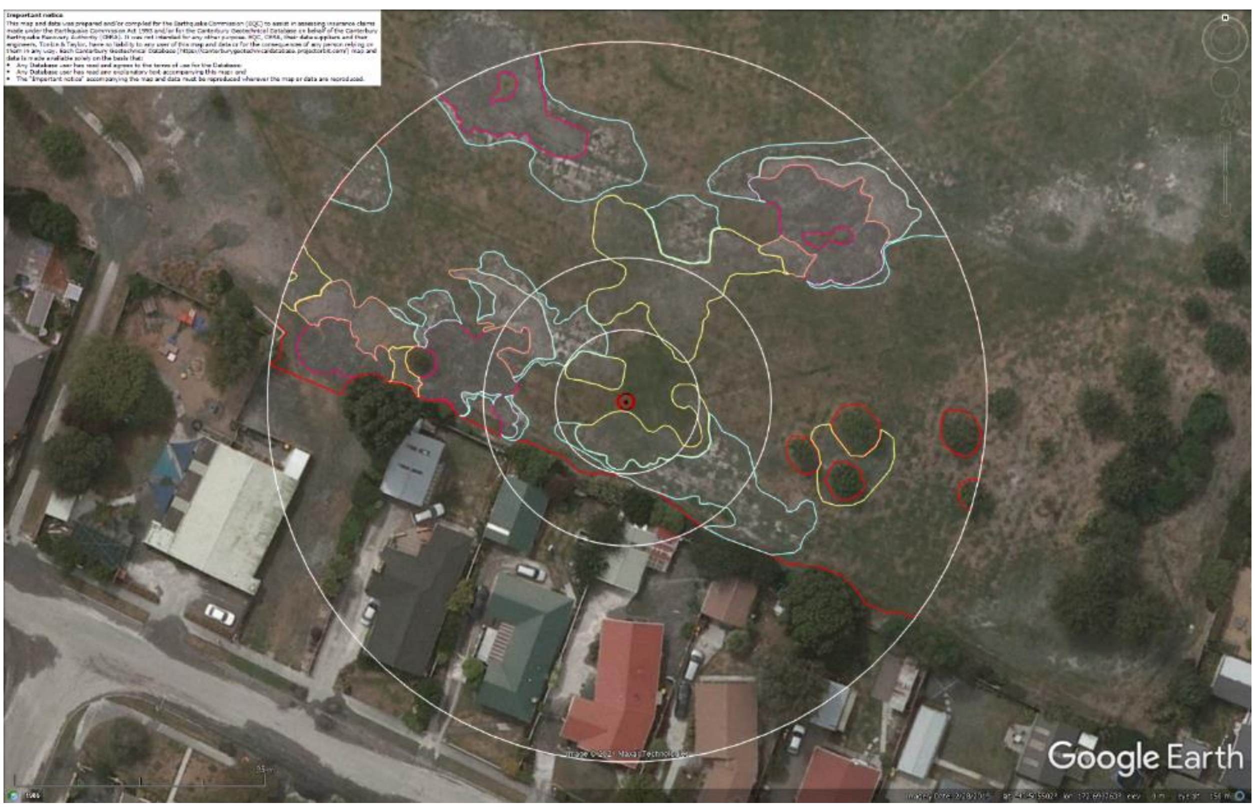

Figure 36: Aerial photograph showing the ejecta outline at the site for Feb-11 EQ.

Figure 37: Aerial photograph acquired on 14-15 Jun 2011 showing the ejecta outline at the site for Jun-11 EQ.

Figure 38: Aerial photograph showing the ejecta outline at the site for Dec-11 EQ.

Figure 39: Ground photograph showing remnants of ejecta at a nearby property (photograph date: Aug 2011).

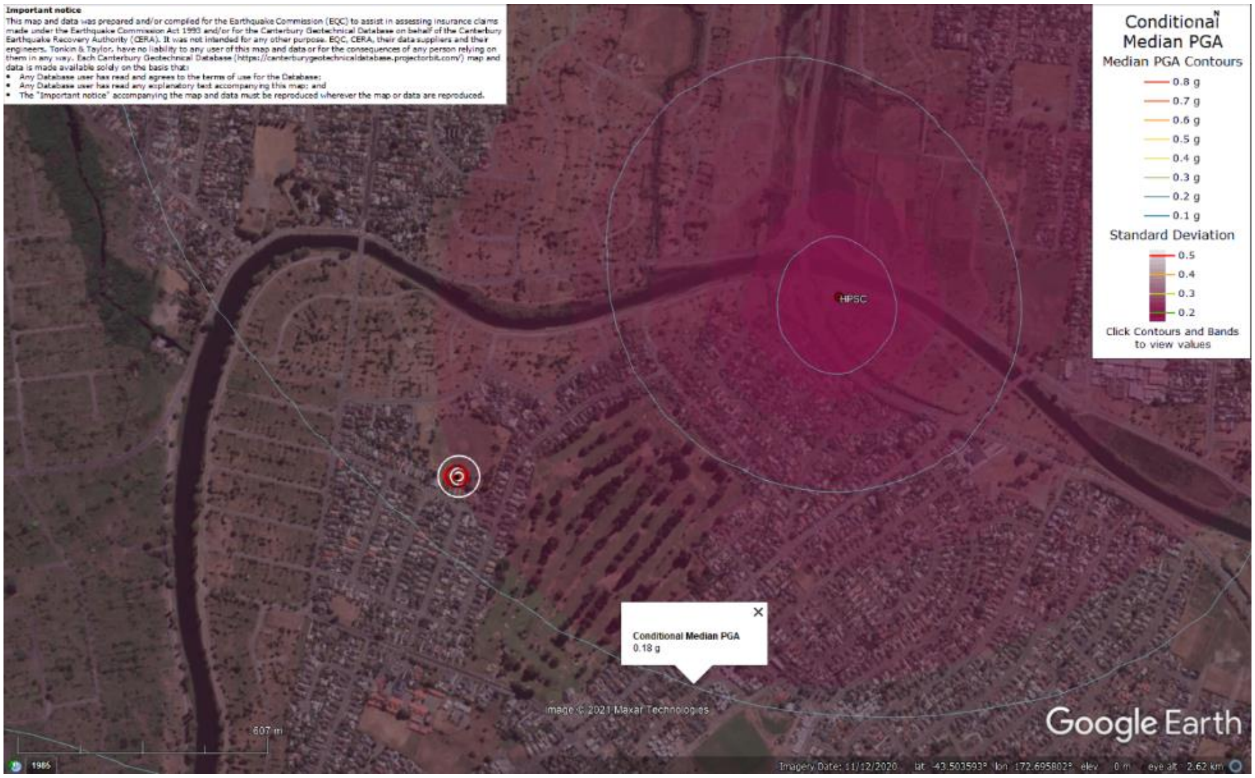

Figure 40: PGA for Sep-10 EQ (st. dev. = 0.275-0.325 ln units).

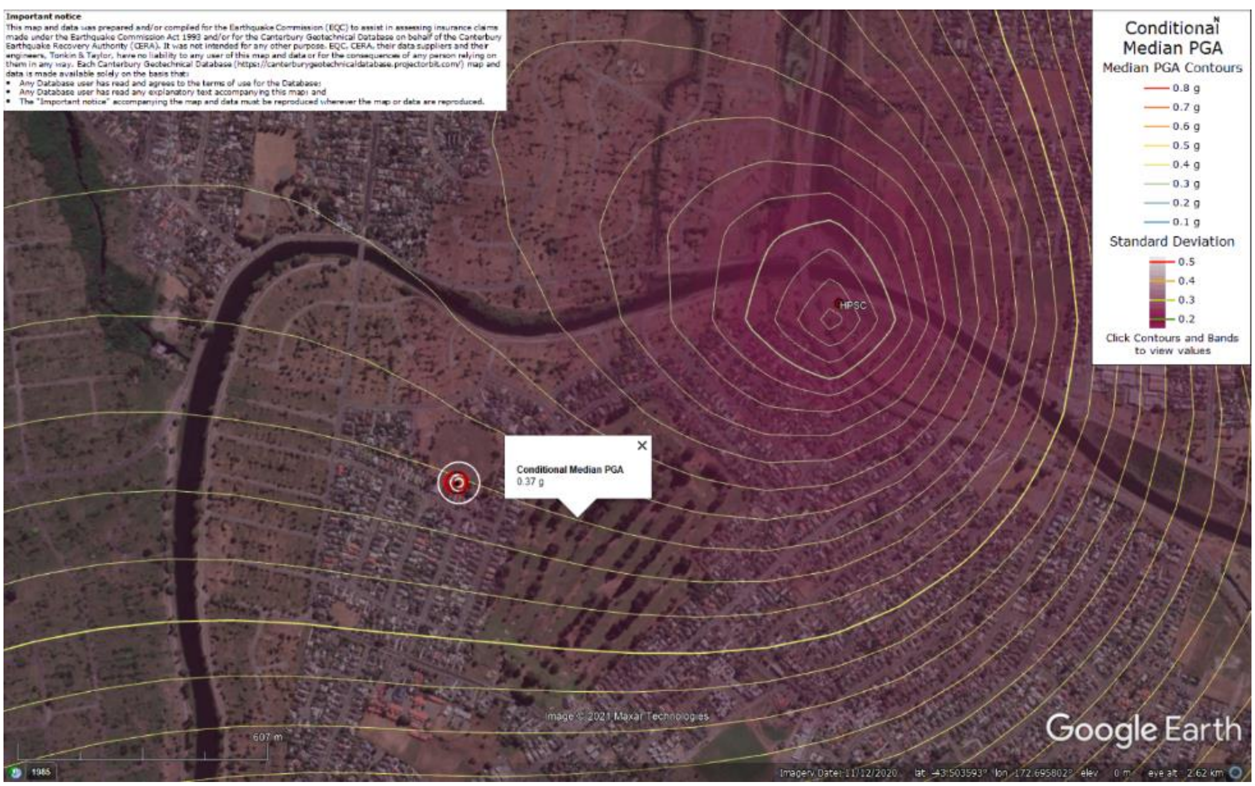

Figure 41: PGA for Feb-11 EQ (st. dev. = 0.300-0.325 ln units).

Figure 42: PGA for Jun-11 EQ (st. dev. = 0.325-0.350 ln units).

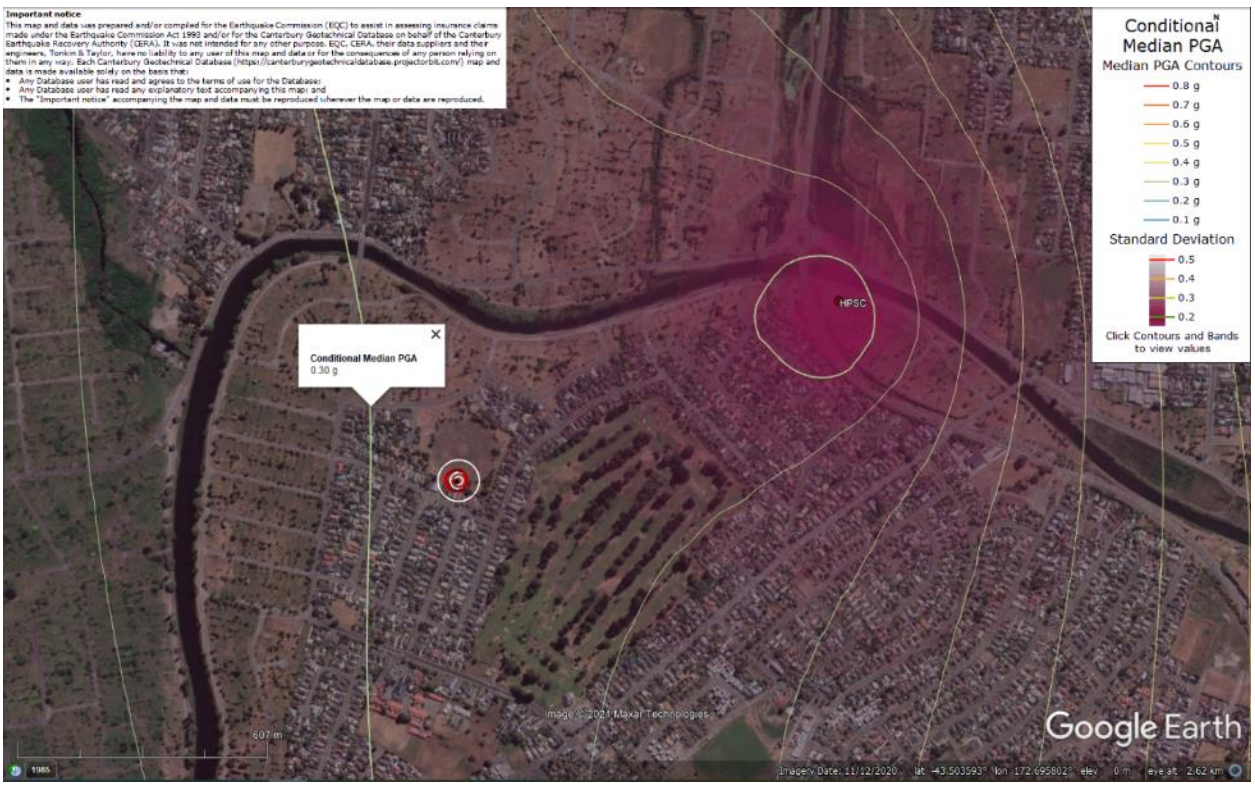

Figure 43: PGA for Dec-11 EQ (st. dev. = 0.325-0.375 ln units).

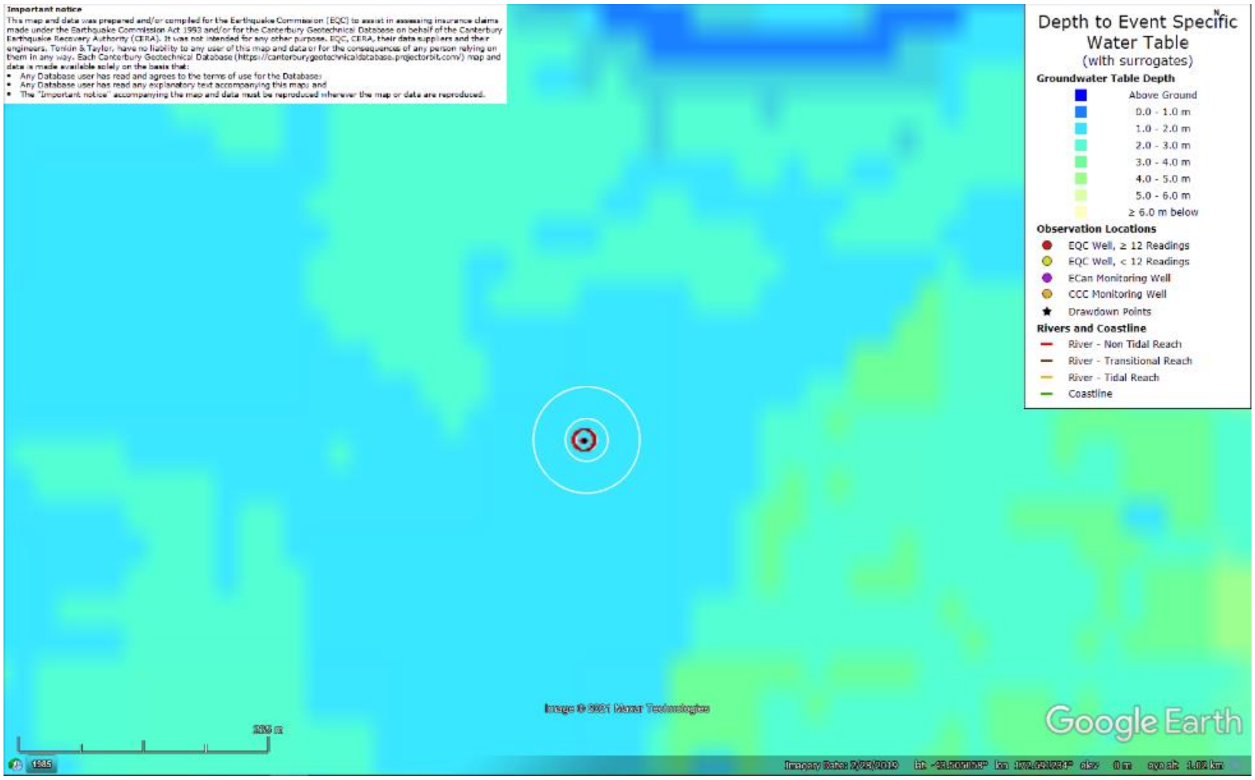

Figure 44: Depth to groundwater table for Sep-10 EQ.

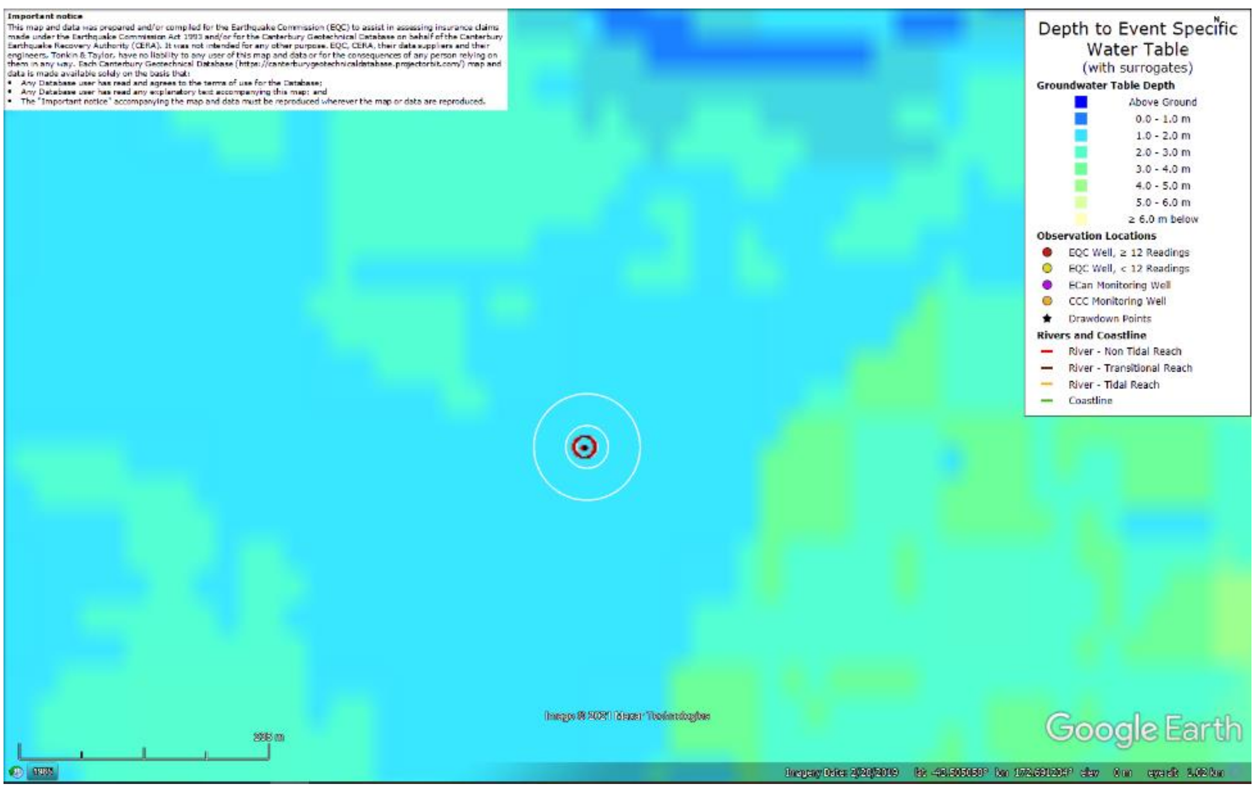

Figure 45: Depth to groundwater table for Feb-11 EQ.

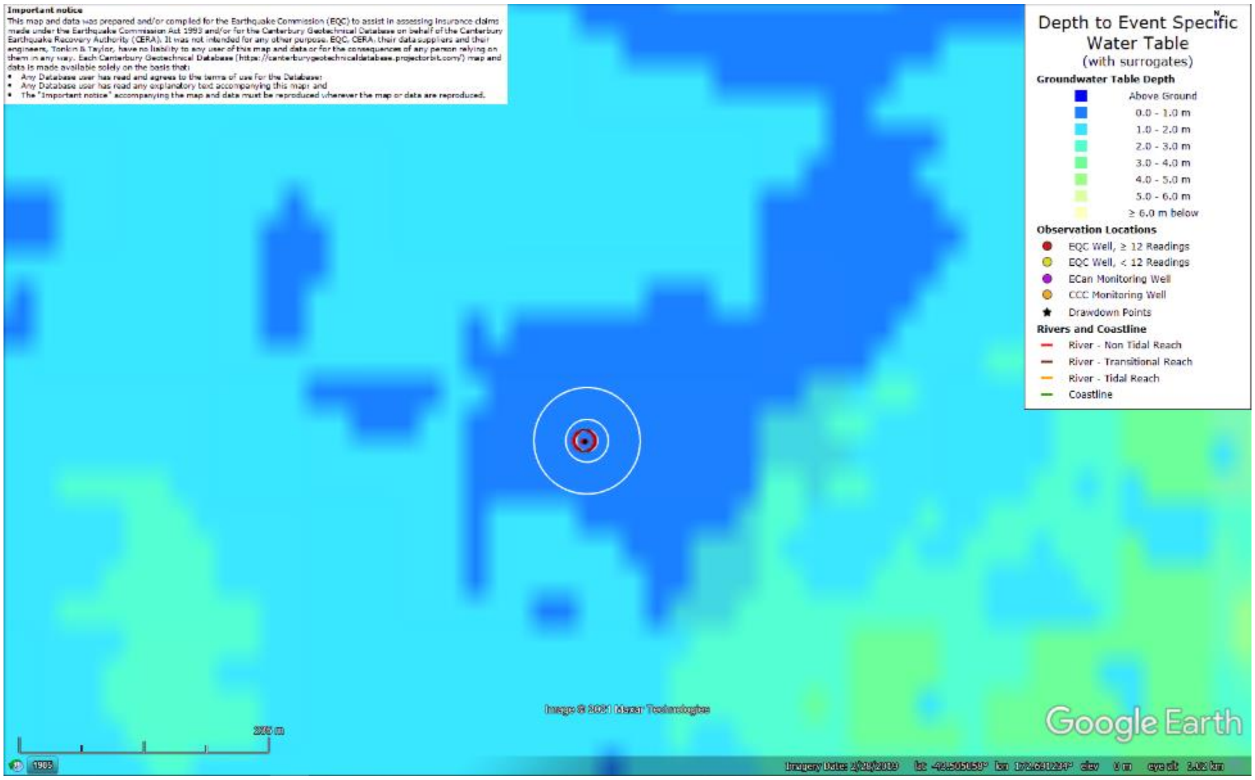

Figure 46: Depth to groundwater table for Jun-11 EQ.

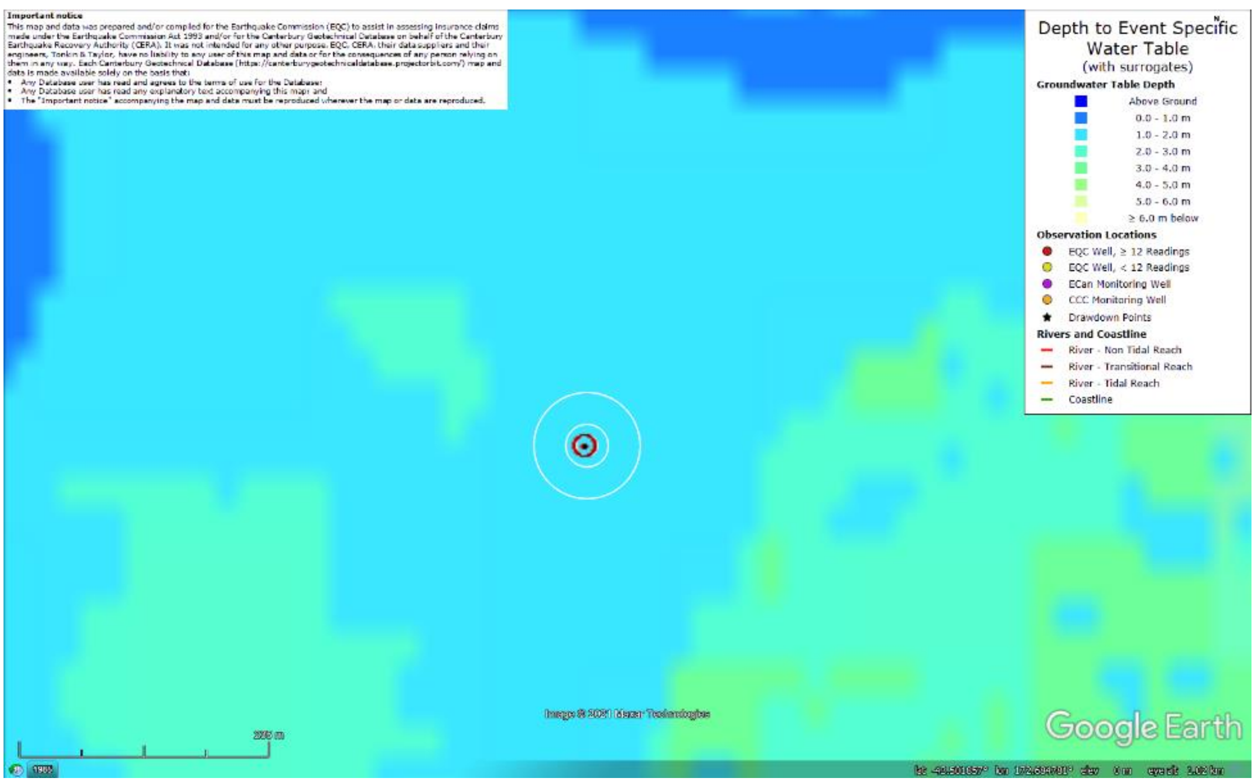

Figure 47: Depth to groundwater table for Dec-11 EQ.

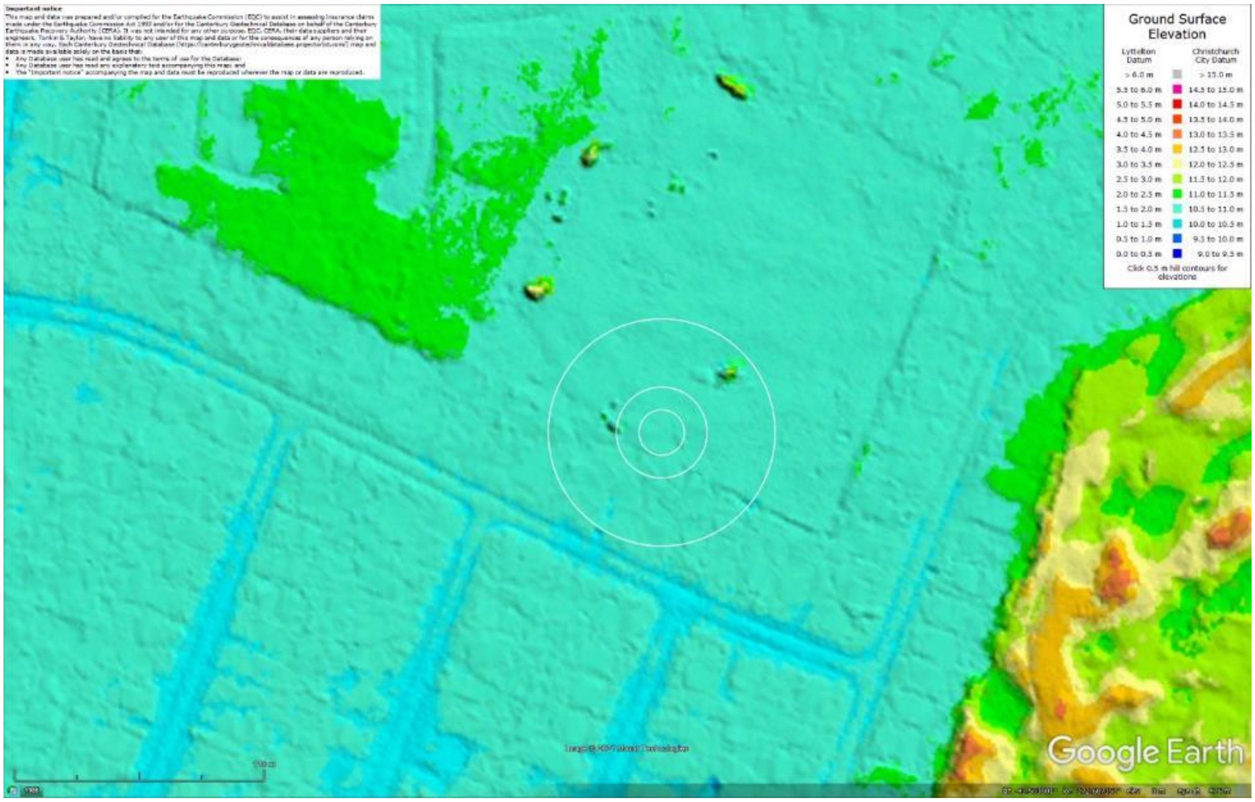

Figure 48: Ground surface elevation according to the Sep-11 LiDAR survey.

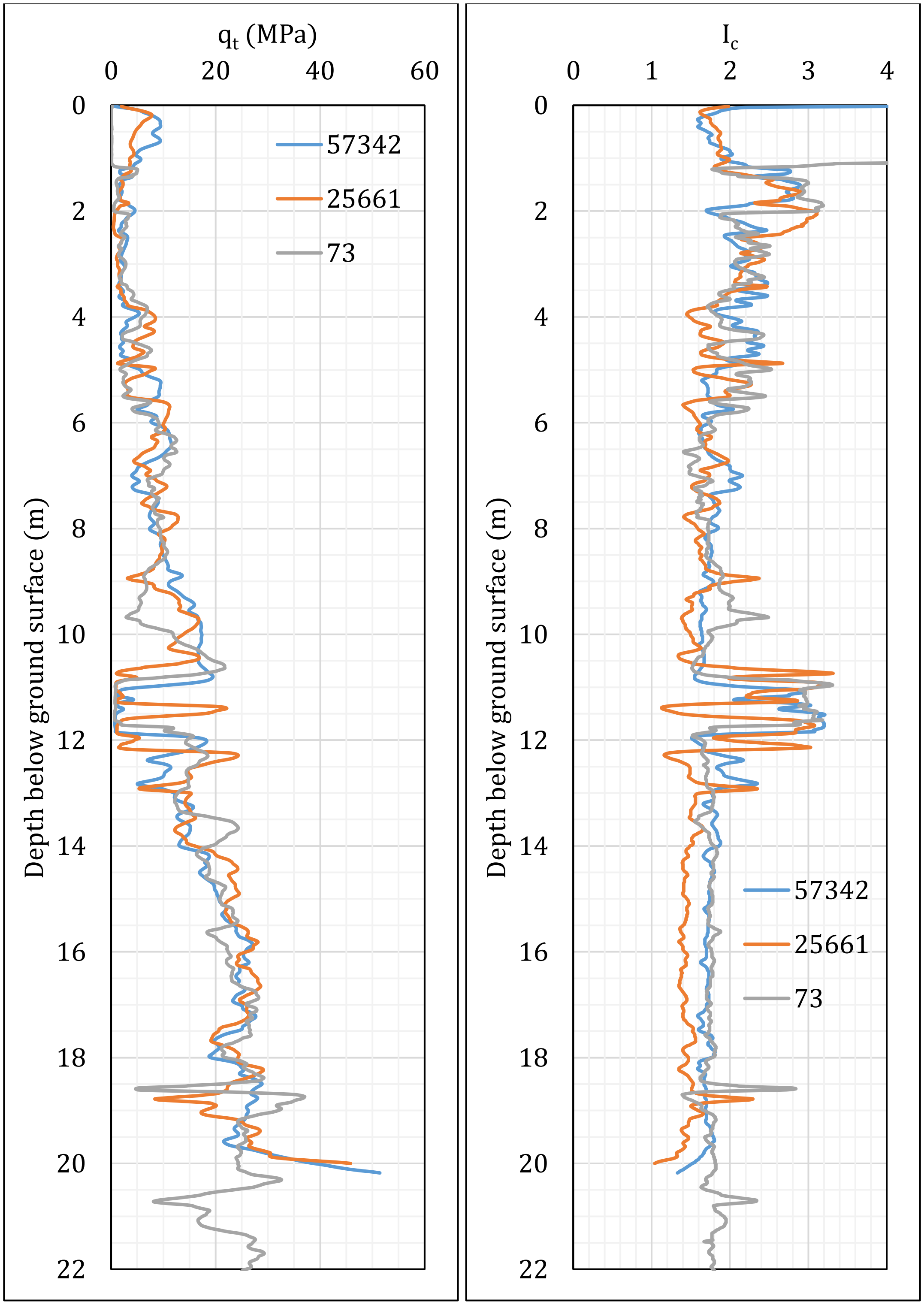

Figure 49: q_t and I_c profiles.

Note 5: The selection of CPTs for the area considered for settlement assessment (Figure 1) is based on the proximity of the CPTs to the considered areas. In accordance with that, the following table shows CPTs that were used for the volumetric settlement analysis in Cliq v.3.0.3.2, a CPT soil liquefaction software developed by GeoLogismiki. (The average volumetric settlements were reported in Table 8.)

Table 12: CPT profiles used in volumetric settlement analysis for areas selected for settlement assessment.

CPT ID No.	10-m buffer	20-m buffer	50-m buffer
57342 (56582)	✓	✓	✓
25661		✓	✓
73			✓

Table 13: CPT-based results.

		CPT ID		
EQ Event	Parameter	57342	25661	73
Sep-10	S_{V1D} (mm)	41	80	60
	LSN	9	15	11
	LPI	1	2	1
	LPI_{ish}	0	0	0
	$D_{FS<1}$ (m)	4.24	2.80	4.89
Feb-11	S_{V1D} (mm)	154	182	174
	LSN	35	33	35
	LPI	17	21	20
	LPI_{ish}	4	12	4
	$D_{FS<1}$ (m)	1.88	2.46	2.02
Jun-11	S_{V1D} (mm)	124	164	148
	LSN	31	40	33
	LPI	11	15	15
	LPI_{ish}	9	9	11
	$D_{FS<1}$ (m)	1.94	1.08	2.02
Dec-11	S_{V1D} (mm)	122	154	144
	LSN	29	29	30
	LPI	10	13	12
	LPI_{ish}	6	8	7
	$D_{FS<1}$ (m)	1.96	2.46	2.02

Notes: $D_{FS<1}$ = Depth to the first liquefiable layer (FS_L<1) that is at least 200-mm thick, as determined by the Boulanger and Idriss (2016) liquefaction-triggering procedure (P_L=50%, C_{FC}=0.13, and $I_{c,cutoff}$ =2.6), and exported from *Cliq v.3.0.3.2*; undet. = the specified soil layer was not detected.

Note 6: Based on the borehole log (BH 57237, Figure 1), the groundwater table is at a depth of 1.4 m below the ground surface. The soil profile consists of (1) sandy fill (SP) to a depth of 0.85 m, (2) organic silty topsoil (OL) to a depth of 1.2 m, (3) silt, ML, of the Christchurch formation to a depth of 2.4 m, (4) silty fine sand, SM, of the Christchurch formation to a depth of 2.9 m, (5) fine to medium sand, SP, of the Christchurch formation to a depth of 3.5 m, (6) silt, ML, to a depth of 3.25 m, (7) fine sand, SP, of the Christchurch formation to a depth of 4.5 m, (8) silt, ML, of the Christchurch formation to a depth of 5.05 m, (9) fine to medium sand, SP, of the Christchurch formation to a depth of 11.3 m, (10) silt, ML, of the Christchurch formation to a depth of 11.95 m, and (11) fine to medium sand, SP, of the Christchurch formation to a depth of 17.15 m. The sandy fill might be a result of the earthwork following the Jun-11 earthquake.

Note 7: The ejecta-induced free-field settlement provided in Table 11 is an areal average settlement due to ejecta, which is based on the total settlement assessment area, A_T (provided in Table 9 and repeated in Table 14). However, the considered area was not always covered completely with ejecta; thus, it is important to provide the localized ejecta-induced settlement, too. The localized settlement due to ejecta is estimated using photographic evidence only as

$$S_{E,P\_localized} = \frac{V_E}{A_E}$$

where V_E is the total volume of ejecta within A_T and A_E is the total coverage area of ejecta within A_T. Please note that the areal ejecta-induced settlement provided in Table 14 as S_{E,P_areal} is the same as $S_{E,P}$ in Table 11, which was estimated as

$$S_{E,P\_areal} = S_{E,P} = \frac{V_E}{A_T}$$

where V_E is the total volume of ejecta within A_T and A_T is the total settlement assessment area.

Table 14a: Areal and localized ejecta-induced settlement estimates for Patch A (10-m buffer) based on photographic evidence.

Earthquake Event	A_T (m²)	A_E (m²)	V_E (m³)	S_{E,P_areal} (mm)	$S_{E,P\_localized}$ (mm)
Sep-10	314	0	0	0	0
Feb-11	314	143	2.6-5.2	15±5	30±10
Jun-11	314	26.2	1.5-2.5	5±5	80±20
Dec-11	161	17.1	0.05-0.1	<5	5±5

Notes: S_{E,P_areal} = $S_{E,P}$ reported in Table 11 = areal ejecta-induced settlement; $S_{E,P\_localized}$ = localized ejecta-induced settlement; A_T = total settlement assessment area; V_E = total volume of ejecta within A_T; A_E = total area of ejecta within A_T; The estimates of both areal and localized ejecta-induced settlement are rounded to the nearest 5; Final plus/minus values are also rounded to the nearest 5.

Table 14b: Areal and localized ejecta-induced settlement estimates for Patch A (20-m buffer) based on photographic evidence.

Earthquake Event	A_T (m²)	A_E (m²)	V_E (m³)	S_{E,P_areal} (mm)	$S_{E,P\_localized}$ (mm)
Sep-10	1035	0	0	0	0
Feb-11	1035	525	12.2-24.4	20±5	35±10
Jun-11	1026	48.0	2.8-4.7	5±5	80±20
Dec-11	733	48.1	1.0-1.5	<5	25±5

Notes: S_{E,P_areal} = $S_{E,P}$ reported in Table 11 = areal ejecta-induced settlement; $S_{E,P\_localized}$ = localized ejecta-induced settlement; A_T = total settlement assessment area; V_E = total volume of ejecta within A_T; A_E = total area of ejecta within A_T; The estimates of both areal and localized ejecta-induced settlement are rounded to the nearest 5; Final plus/minus values are also rounded to the nearest 5.

Table 14c: Areal and localized ejecta-induced settlement estimates for Patch A (50-m buffer) based on photographic evidence.

Earthquake Event	A_T (m²)	A_E (m²)	V_E (m³)	S_{E,P_areal} (mm)	$S_{E,P\_localized}$ (mm)
Sep-10	4905	0	0	0	0
Feb-11	4905	1947	67.5-135	20±10	50±15
Jun-11	4822	485	28.2-47.1	10±5	80±20
Dec-11	4572	501	20.3-37.0	5±5	60±15

Notes: S_{E,P_areal} = $S_{E,P}$ reported in Table 11 = areal ejecta-induced settlement; $S_{E,P\_localized}$ = localized ejecta-induced settlement; A_T = total settlement assessment area; V_E = total volume of ejecta within A_T; A_E = total area of ejecta within A_T; The estimates of both areal and localized ejecta-induced settlement are rounded to the nearest 5; Final plus/minus values are also rounded to the nearest 5.

Summary 2:

The best estimate of the localized ejecta-induced free-field ground settlement at the Avondale Park site for the SEP 2010, FEB 2011, JUN 2011, and DEC 2011 earthquake is 0 mm, 50±15 mm, 80±20 mm, and 60±15 mm, respectively.